Program Digest, 2019 IEEE International Ultrasonics Symposium (IUS)
Glasgow, Scotland, October 6-9, 2019

Integrated Ultrasound and Photoacoustic Imaging for Effective Endovenous Laser Ablation: A Characterization Study

Samuel John
Biomedical Engineering
Wayne State University
Detroit, MI, United States
gd1321@wayne.edu

Yan Yan
Biomedical Engineering
Wayne State University
Detroit, MI, United States
yyan2@wayne.edu

Shmuel Yeshya Forta
Biomedical Engineering
Wayne State University
Detroit, MI, United States
fw0631@wayne.edu

Loay Kabbani
Vascular Surgery
Henry Ford Hospital
Detroit, MI, United States
LLKABBANI@hfhs.org

Mohammad Mehrmohammadi
Biomedical Engineering
Wayne State University
Detroit, MI, United States
mehr@wayne.edu

***Abstract*— Chronic venous insufficiencies due to venous valvular incompetence cause varicose veins. Varicose are characterized by the superficial bulging varicosities and are responsible for a variety of ailments, including pain, bleeding, dermatitis and even venous ulcers. Endovenous laser ablation (EVLA) is a minimally invasive, ultrasound (US)-guided procedure for treating varicose veins. However, US imaging suffers from artifacts and is unable to visualize the accurate location of the fiber tip within the vein. Current clinical EVLA procedures lack the ability to monitor the real-time temperature inside the vein during ablation procedures. Photoacoustic (PA) imaging can be integrated with existing EVLA systems for accurate fiber tip tracking and real-time temperature monitoring. This study will focus on characterizing the effectiveness of the PA-guided fiber tip tracking procedures at (1) different depths of the vessel, (2) different fiber orientations and different pulsed laser energies. The temperature monitoring capabilities of PA imaging will be evaluated using a real-world**

Keywords*— *ultrasound, photoacoustic, venous insufficiencies, ablation, laser, temperature

I. Introduction

Chronic venous insufficiency (CVI) is a prevalent condition that contributes to the development of varicose veins. Varicose veins affect more than 40 million people in the United States. The treatment costs for CVI has been estimated to vary from $750 million to $1 billion a year in the Unites States [1]. Varicose veins are characterized superficial twisted and bulged veins caused by the accumulation of blood due to loss of venous elasticity [2]. Due to the high success rate and short recovery time, endovenous laser ablation (EVLA) is used for treating varicose veins [3, 4]. In EVLA, an ultrasound [5] (US)-guided fiber carrying high power continuous wave (CW) laser energy is placed within the diseased vein. The localized heat generated at the tip of the fiber interacts with the vein wall and seals the vein. [6]. However, US imaging suffers from angular dependency [7-9] and sometimes is unable to visualize the accurate location of the fiber within the vein **(Fig. 1a)**. In perforator veins, poor fiber visualization leads to the cauterization at the incorrect vein location and leads to the formation of deep vein thrombosis in deep veins [10]. Also, operator-related errors [7] and reverberation artifacts limit the efficacy of US-guided EVLA procedures [7]. Current clinical EVLA systems lack a temperature feedback system to monitor the real-time thermal dose deposition and thus accurate formation of the thermal lesion [6]. Hence, EVLA procedures performed without any temperature monitoring and may lead to an insufficient thermal dose which may cause the recurrence of varicose veins or recanalization [11]. In addition, excessive thermal dosage may lead to vein wall perforations [12]. This damages the pervious tissue surrounding the treated vein and causes endovenous heat induced thrombosis (HIT) [13] (1-2%), ecchymosis [6, 12, 13].

To overcome these limitations, we envision to integrate photoacoustic (PA) imaging with current EVLA system for accurate fiber tip tracking and real-time temperature monitoring. PA imaging utilizes short (ns), non -ionizing laser pulses to excite the surrounding medium [14, 15]. The excited tissue undergoes thermoelastic expansion and releases acoustic waves. These acoustic waves are detected using an US transducer. Since the PA signal is generated at the interface between the fiber tip and the surrounding medium, it indicates the accurate location of the fiber tip **(Fig. 1b)** [7-9]. The natural co-registration between US and PA images will potentially help the vascular surgeons to visualize the accurate location of the fiber tip within the background vasculature **(Fig. 1c)**. Since the amplitude of the PA signal is proportional to surrounding temperature [16], PA imaging can be used for monitoring the real-time temperature inside the diseased vein.

Michigan Translational Research and Commercialization Fund (MTRAC)

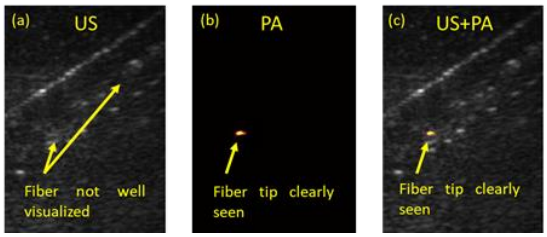

Figure 1: (a) Due to angular dependency and low contrast to noise ratio, US imaging fails to visualize the fiber tip. (b) PA imaging visualizes the fiber tip only. (c) US/PA imaging tracks the fiber within the background tissue.

II. MATERIALS AND METHODS

A. *Principles of PA imaging for fiber tracking and temperature monitoring.*

A fiber carrying short (in the order of nanoseconds), non-ionizing laser pulses placed within a diseased vein. The energy of these laser pulses is absorbed by the blood surrounding the fiber and is converted into heat, which causes thermoelastic expansions within the blood molecules. These expansions give rise to spherical acoustic waves which travel omnidirectionally and are detected by the US transducer. The PA signal is defined by:

$$P = \Gamma \mu a F \quad (1)$$

where Γ corresponds to the Grüneisen parameter, μa is denoted as the absorption coefficient and laser fluence is denoted by F. The Grüneisen coefficient is defined by:

$$\Gamma(T) = (\beta c^2)/Cp\,(T) \quad (2)$$

where β is the thermal coefficient of volume expansion, c corresponds to the speed of sound and Cp is the heat capacity at constant pressure.

$$\Delta T = a\Delta P/P \quad (3)$$

where $\Delta P/P$ refers to the relative amplitude of the PA signal, a refers to the temperature dependent constant and ΔT refers to the change in temperature of the surrounding medium.

B. *Integrated PA/ EVLA system*

An integrated system **(Fig. 2)** was designed by combining the pulsed laser beam (λ = 532 nm, repetition rate of 10Hz, PA imaging) from a pulsed laser (Anderson Lasers Inc., Ohio , USA) and the continuous wave laser beam (λ = 1470 nm, ablation) from a continuous wave laser (Venacure, Angiodynamics, New York, USA), through a dichroic mirror (Newport, USA) into an ablation fiber [7, 9]. The dichroic mirror combines the beam by reflecting the visible wavelengths (λ = 400-700 nm) and transmitting the near infra-red wavelengths (780-2500 nm). The strong absorption of blood at λ = 532 nm enables the selected wavelength suitable for PA imaging. The addition of low-cost optics and low-cost pulsed laser provides a cost-effective solution to enhance EVLA procedures. Integration of PA imaging with EVLA procedures does not draw any safety concerns because the power of the pulsed laser is lower than the CW ablation laser.

Integration of PA imaging with clinical EVLA systems can be designed with minimal system modifications because the (1) the same ablation fiber carries the combined beam into the diseased vein, (2) The same US transducer can be used for acquiring US and PA signals, (3) US and PA images can be easily co-registered to provide accurate images of the fiber tip and (4) The same fiber be used for monitoring the temperature inside the diseased vein [7].

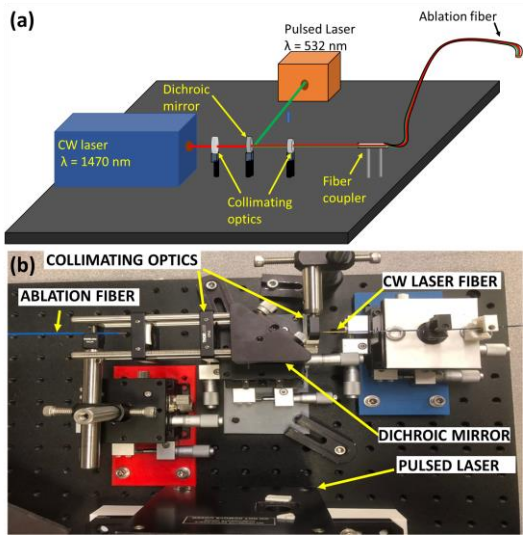

Figure 2: (a) Schematic of the integrated PA/ EVLA system. (b) Experimental setup of the integrated PA/ EVLA system for accurate fiber tip tracking and real-time temperature monitoring.

C. *PA imaging for catheter's tip tracking characterization studies*

The ability of PA imaging to track the fiber tip at different depths with different pulse energies was evaluated by placing a fiber (1000 µm diameter, NeverTouch, Angiodynamics, New York, USA) carrying the combined beam (λ = 532 nm, and λ = 1470 nm) inside an US transparent tube (diameter - 0.5 cm) filled with heparinized sheep blood (Cedarlane, Canada) and placed within a vessel-mimicking porcine background **(Fig. 3a)**. The imaging system consisted of a 128-element linear array transducer (L7-4, Verasonics, Kirkland, USA) and a programmable digital US research platform (Vantage 64, Verasonics, Kirkland, USA). Sagittal US/PA images of the fiber tip were acquired at different depths (1, 2, 3 cm) and different pulsed laser energies (50, 100, 150 µJ) respectively. The ability of PA imaging to track the fiber at different fiber orientations and different pulse energies was evaluated by placing the fiber carrying a combined beam inside an US transparent tube (diameter – 0.5 mm) filled with heparinized sheep blood, and placed inside an imaging tank filled with water **(Fig. 3b)**. Sagittal US/PA images of the fiber tip were acquired at different fiber orientations (10^0 - 35^0) and different laser energies (50, 100, 150 µJ) respectively. The experiment was performed at a constant imaging depth of 3 cm .

D. *In vivo real-time PA thermometry in a canine model*

The ability of PA imaging to monitor the real-time temperature was simulated by placing the fiber carrying the combined beam (λ = 532 nm, pulse energy of 200 µJ and λ = 1470 nm) inside the jugular vein of a live canine model **(Fig.**

3c). The input CW laser energy was 12W. The combined beam at the fiber contained substantial CW laser energy for ablation. A K-type thermocouple (temperature range of 0 to 200^{0}C) was placed near the fiber tip to monitor the variations in temperature inside the vein due to the ablation laser. Transverse US/PA images of the fiber tip were acquired.

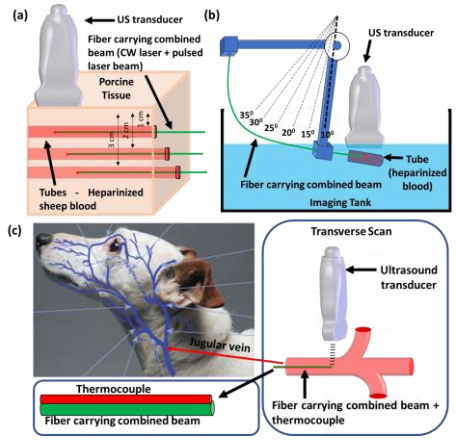

Figure 3: (a) Experimental setup for tracking the fiber tip at different pulsed laser energies at different depths (b) different fiber orientations. (c) Experimental setup to evaluate the real-time temperature monitoring capability of PA imaging in a live animal (canine) model.

III. RESULTS AND DISCUSSIONS

A. PA imaging to track the fiber at different depths at different pulsed laser energies.

Figure 4 shows the variation of the PA amplitude at different pulsed laser energies, when placed at different vessel depths inside the phantom. The error bars indicate the standard deviation along each measurement. The graph indicates that the PA amplitude at 50 µJ, placed at a depth of 3 cm, is still detectable and does not change significantly, when compared with the PA amplitude with 150 µJ at the same depth. These amplitude variations with different energies at a constant depth are accounted for by the change in fluence (increasing laser energy over a small fixed region in front of the fiber) (1). The decrease in the PA amplitude at the same energy with increasing depth is due to the attenuation of the acoustic waves by the porcine tissue. This study envisions the possibility of utilizing a low power pulsed laser for fiber tracking capabilities.

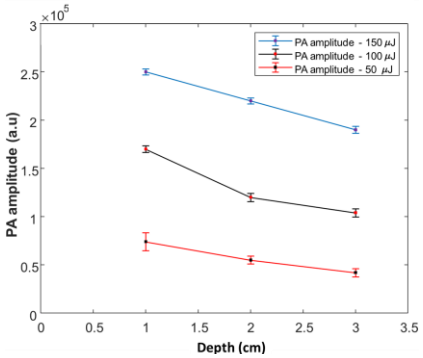

Figure 4: PA imaging of the fiber tip carrying a combined beam with different pulse energies inside US transparent tubes within a porcine tissue vessel-mimicking phantom.

B. PA imaging to track the fiber at different fiber oreintations at different pulsed laser energies

Figure 5 demonstrates the ability of PA imaging to track the fiber with different pulse energies at different fiber orientations. The PA imaging detects the fiber tip at all orientations because the PA signal generated at the tip of the fiber travels omnidirectionally and is picked up by the US transducer. However, US loses the fiber tip at an angle of 30^0 because the echoes reflected from the fiber move away from the US imaging plane. The PA amplitude with constant energy at various angles in a water medium is not attenuated significantly as compared to the porcine tissue. This characterization graph indicates the superior ability of PA imaging to track the fiber at all fiber orientations, (especially in the perforator veins) and will potentially minimize complications.

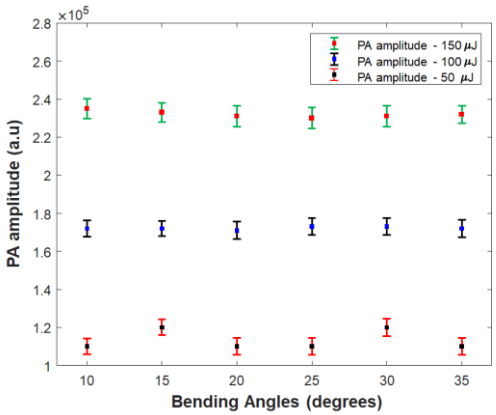

Figure 5: PA imaging of the fiber tip carrying a combined beam with different pulse energies at different fiber orientations placed inside a US transparent tube at a constant depth of 3cm.

C. Real-time PA thermometry in a live canine model

Figure 6 validates the superior ability of PA imaging to monitor the changes in the real-time temperature inside the jugular vein of a live canine model under anesthesia. The PA amplitude varies with the change in the surrounding temperature caused by the localized heat generated by the ablation fiber (3). At higher temperatures, it is expected that the optical properties of blood changes. It is reported at temperatures above 50^{0}C, the tissue becomes denatured, the Grüneisen parameter is altered in a nonlinear fashion [17-19]. In addition, it is known that optical properties of blood (absorption and scattering) varies with change in its temperature. Studying the temperature-dependent variations in optical properties of blood (μ_a) is the subject of our ongoing research. Having such priori information on relationship between blood absorption coefficients at different temperatures will allow for performing quantitative PA thermometry where the relation between the surrounding temperature and the PA signal changes can be accurately calculated. This calibration studies will provide a relationship between the change in the PA signal and temperature change in blood and the surrounding tissue. Since the fluence of pulsed laser light can be considered relatively constant, such calibration studies can be used to monitor the temperature changes during ablation, independent from the location and size of the ablated veins (in contrast to externally illuminated PA thermometry). The PA-guided thermometry inside the diseased vein during

EVLA procedures will potentially reduce complications and will significantly shorten the duration of the surgery.

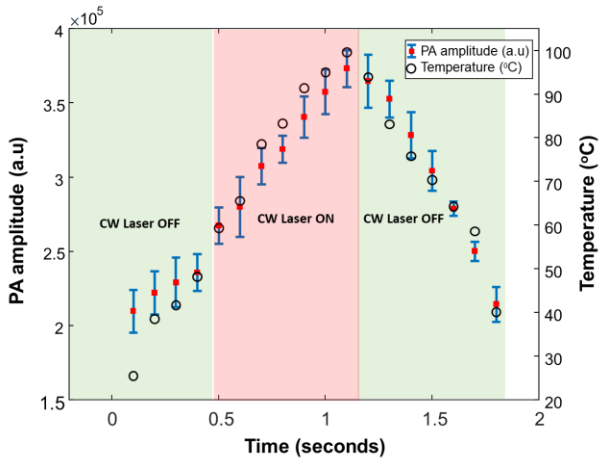

Figure 6: Changes in PA amplitude vs. increase in temperature inside the vein caused by the CW laser. Green panels indicate the duration when the CW laser was turned OFF and the red panel indicates the duration when the CW laser was turned ON.

IV. CONCLUSION

Future work will involve the comparative study between standalone US and US/PA-guided fiber tip tracking in the perforator veins of a live canine model. The ability of PA imaging in tracking the fiber tip at different depths, fiber orientations and pulse energies has been studied and characterized through a set of vessel-mimicking experiments. The ability of PA imaging to monitor the real-time temperature changes caused by a clinical CW laser has been validated through a live canine model. The intensity of the PA signal correlates with the increase in temperature of the surrounding medium. The integrated system can potentially enhance EVLA procedures and will improve the healthcare for patients with venous insufficiencies.

V. ACKNOWLEDGMENT

The authors would like to acknowledge Mr. Sumanth Putta of Wayne State University for his valuable help in performing the experiments, Ms. Josie Beck from Angiodynamics for providing the CW laser for the animal studies and Ms. Carol Bridge and Dr. Hani Sabbah from Henry Ford Health Systems for her valuable help in assisting with the animal studies

VI. REFERENCES

[1] M. S. Weingarten, "State-of-the-art treatment of chronic venous disease," Clinical infectious diseases, pp. 949-954, 2001.

[2] R. H. Jones and P. J. Carek, "Management of varicose veins," American family physician, vol. 78, no. 11, 2008.

[3] R. Balint et al., "Which endovenous ablation method does offer a better long-term technical success in the treatment of the incompetent great saphenous vein? Review," Vascular, vol. 24, no. 6, pp. 649-657, 2016.

[4] G. Galanopoulos and C. Lambidis, "Minimally invasive treatment of varicose veins: Endovenous laser ablation (EVLA)," International Journal of Surgery, vol. 10, no. 3, pp. 134-139, 2012.

[5] S. Elias and E. Peden, "Ultrasound-guided percutaneous ablation for the treatment of perforating vein incompetence," Vascular, vol. 15, no. 5, pp. 281-289, 2007.

[6] R. R. van den Bos, M. A. Kockaert, H. M. Neumann, R. H. Bremmer, T. Nijsten, and M. J. van Gemert, "Heat conduction from the exceedingly hot fiber tip contributes to the endovenous laser ablation of varicose veins," Lasers in medical science, vol. 24, no. 2, pp. 247-251, 2009.

[7] S. John, V. Yan, L. Kabbani, N. A. Kennedy, and M. Mehrmohammadi, "Integration of Endovenous Laser Ablation and Photoacoustic Imaging Systems for Enhanced Treatment of Venous Insufficiency," in 2018 IEEE International Ultrasonics Symposium (IUS), 2018, pp. 1-4: IEEE.

[8] Y. Yan, S. John, M. Ghalehnovi, L. Kabbani, N. A. Kennedy, and M. Mehrmohammadi, "Ultrasound and photoacoustic imaging for enhanced image-guided endovenous laser ablation procedures," in Medical Imaging 2018: Ultrasonic Imaging and Tomography, 2018, vol. 10580, p. 105800T: International Society for Optics and Photonics.

[9] Y. Yan, S. John, M. Ghalehnovi, L. Kabbani, N. A. Kennedy, and M. Mehrmohammadi, "photoacoustic Imaging for Image-guided endovenous Laser Ablation procedures," Scientific reports, vol. 9, no. 1, p. 2933, 2019.

[10] N. Kurihara, M. Hirokawa, and T. Yamamoto, "Postoperative venous thromboembolism in patients undergoing endovenous laser and radiofrequency ablation of the saphenous vein," Annals of vascular diseases, vol. 9, no. 4, pp. 259-266, 2016.

[11] W. Malskat, M. Stokbroekx, C. van der Geld, T. Nijsten, and R. Van den Bos, "Temperature profiles of 980-and 1,470-nm endovenous laser ablation, endovenous radiofrequency ablation and endovenous steam ablation," Lasers in medical science, vol. 29, no. 2, pp. 423-429, 2014.

[12] R. R. Van Den Bos, M. Neumann, K. P. DE ROOS, and T. Nijsten, "Endovenous laser ablation–induced complications: review of the literature and new cases," Dermatologic Surgery, vol. 35, no. 8, pp. 1206-1214, 2009.

[13] S. J. Rhee, N. L. Cantelmo, M. F. Conrad, and J. Stoughton, "Factors influencing the incidence of endovenous heat-induced thrombosis (EHIT)," Vascular and endovascular surgery, vol. 47, no. 3, pp. 207-212, 2013.

[14] M. Mehrmohammadi, S. Joon Yoon, D. Yeager, and S. Y Emelianov, "Photoacoustic imaging for cancer detection and staging," Current molecular imaging, vol. 2, no. 1, pp. 89-105, 2013.

[15] P. Beard, "Biomedical photoacoustic imaging," Interface focus, vol. 1, no. 4, pp. 602-631, 2011.

[16] J. Shah et al., "Photoacoustic imaging and temperature measurement for photothermal cancer therapy," Journal of biomedical optics, vol. 13, no. 3, p. 034024, 2008.

[17] F. J. O. Landa, X. L. Deán-Ben, R. Sroka, and D. Razansky, "Volumetric optoacoustic temperature mapping in photothermal therapy," Scientific reports, vol. 7, no. 1, p. 9695, 2017.

[18] I. V. Larina, K. V. Larin, and R. O. Esenaliev, "Real-time optoacoustic monitoring of temperature in tissues," Journal of Physics D: Applied Physics, vol. 38, no. 15, p. 2633, 2005.

[19] R. O. Esenaliev, A. A. Oraevsky, K. V. Larin, I. V. Larina, and M. Motamedi, "Real-time optoacoustic monitoring of temperature in tissues," in Laser-Tissue Interaction X: Photochemical, Photothermal, and Photomechanical, 1999, vol. 3601, pp. 268-275: International Society for Optics and Photonics.